

Using Galaxy Formation Simulations to optimise LIGO Follow-Up Observations

Elisa Antolini¹, Ilaria Caiazzo², Romeel Davé³, Jeremy S. Heyl^{*2}

¹*Dipartimento di Fisica e Geologia, Università degli Studi di Perugia, I-06123 Perugia, Italia*

²*Department of Physics and Astronomy, University of British Columbia, 6224 Agricultural Road, Vancouver, BC V6T 1Z1, Canada*

³*Faculty of Natural Science, University of the Western Cape, Private Bag X17, Bellville 7535, Republic of South Africa*

Accepted —. Received —; in original form —

ABSTRACT

The recent discovery of gravitational radiation from merging black holes poses a challenge of how to organize the electromagnetic follow-up of gravitational-wave events as well as observed bursts of neutrinos. We propose a technique to select the galaxies that are most likely to host the event given some assumptions of whether the particular event is associated with recent star formation, low metallicity stars or simply proportional to the total stellar mass in the galaxy. We combine data from the 2-MASS Photometric Redshift Galaxy Catalogue with results from galaxy formation simulations to develop observing strategies that potentially reduce the area of sky to search by up to a factor of two relative to an unweighted search of galaxies, and a factor twenty to a search over the entire LIGO localization region.

Key words: gravitational waves: Physical Data and Processes – galaxies: distances and redshifts: Galaxies – methods: observational: Astronomical instrumentation, methods, and techniques

1 INTRODUCTION

Particular characteristics of individuals are rarely distributed uniformly over a population. In fact a small fraction of a population, even a few percent, can have the majority of a given attribute. In this paper we will use this property of the population of galaxies to optimize electromagnetic follow-up of gravitational-wave and neutrino transients.

Beginning in September 2015 LIGO started to detect gravitational wave events from the local Universe (Abbott et al. 2016). Even after the addition of the Virgo detector in the Spring 2017, the localization of many initial candidate events on the sky is coarse with the ninety-percent confidence regions covering hundreds or even thousands of square degrees (Kasliwal & Nissanke 2014; Singer et al. 2014; Berry et al. 2015; Abbott et al. 2016). Some events will have much better localisations on the order of tens of square degrees. Either way developing an observing strategy for follow-up is crucial. To understand the host environment, the evolution of the progenitor and to provide tests of cosmology by yielding an independent measurement of the redshift of the source requires an electromagnetic counterpart. On the other hand, what these electromagnetic counterparts should look like and how long they should last are uncertain.

Although many have considered the electromagnetic transients associated with the mergers of binaries that include a neutron star (e.g. East et al. 2016; Kawaguchi et al. 2016; D’Orazio et al. 2016; Fernández & Metzger 2016; Mingarelli et al. 2015; Kyutoku et al. 2015; Siegel & Ciolfi 2016b,a), the first discovered gravitational wave event (GW150914) was almost certainly the merger of binary black holes. In this case there are only a few models (e.g. Gerosa et al. 2015; Margalit & Piran 2015; Cerioli et al. 2016; Yang & Zhang 2016) that hypothesize the appearance and duration of the electromagnetic counterparts. Rapid electromagnetic follow-up of a large portion of the probable region increases the chance of success in finding a potential counterpart, and furthermore, it also increases the likelihood that a potential counterpart indeed accompanied the event. Over the span of days or weeks, many electromagnetic transients typically occur, and with the wide variety of models it will be difficult to associate unambiguously a particular electromagnetic event with a candidate gravitational-wave event.

Here we will build upon the strategy that Antolini & Heyl (2016) pioneered to use the The Two Micron All Sky Survey extended source catalogue (2MASS XSC, Jarrett et al. 2000; Skrutskie et al. 2006) and approximate photometric redshifts from the 2MASS Photometric Redshift (2MPZ) catalogue (Bilicki et al. 2014), to build an efficient observing plan to follow up gravitational wave transients.

* Email: heyjl@phas.ubc.ca; Canada Research Chair

We will use the results of the MUFASA cosmological galaxy formation simulations (Davé et al. 2016b) to find correlations between the calculated 2MASS photometry in the simulations and the properties of the simulated galaxies themselves, total stellar mass, total mass of low-metallicity stars and the current star formation rate. Using these correlations we will create weighted sky maps from the 2MPZ where the values of each pixel are proportional to the total stellar mass, total mass of low- Z stars and star formation rate lying in the given direction over a given redshift range.

2 CALCULATIONS

The objective is to know where to look to increase the probability of finding an electromagnetic counterpart to a gravitational wave event. The modelling and analysis of the gravitational waveform as measured from the LIGO and other sites yields the probability that the observed waveform **data** from the event resulted from a source at a given **position**, $P(\text{data}|\text{position})$ (e.g. Singer & Price 2016), and this information can be combined with a galaxy redshift survey to determine where to look (e.g. Hanna et al. 2014; Bartos et al. 2015; Singer et al. 2016). Here the position includes the location of the source on the sky and in redshift that can be estimated from the gravitational wave detection. Antolini & Heyl (2016) created full sky maps of the galaxy density to estimate $P(\text{position})$ and to construct by Bayes's theorem

$$P(\text{position}|\text{data}) = \frac{P(\text{position})P(\text{data}|\text{position})}{P(\text{data})} \quad (1)$$

where the optimal strategy is to observe those regions of sky where the probability of a source position given the data, $P(\text{position}|\text{data})$, is largest. Antolini & Heyl (2016) were agnostic about which galaxies were most likely to host the event. However, in principle one could associate particular types of gravitational events with particular properties of galaxies. The most conservative approach may be to assume that the merger rate is simply proportional to the total stellar mass of a galaxy, but one could use information about the type of event to optimize the search further. For example, Dominik et al. (2015) argued that the first observed events would come from the merger of black holes with masses of 30-50 solar masses whose progenitors were low metallicity stars. Belczynski et al. (2016) further elaborated on this picture. In this case those galaxies with a large mass of low- Z stars would have a larger probability of harbouring such a source. A contrasting point of view is that the black holes are primordial (e.g. Sasaki et al. 2016). In this case, the events would not be correlated with galaxies at all. O'Shaughnessy et al. (2017) examine in detail how the properties and evolution of a galaxy affect in the rate of compact object mergers in the galaxy. On the other hand, the formation of neutron stars in supernovae could generate bursts of gravitational waves that differ from in-spirals (e.g. Burrows & Hayes 1996; Ott 2009; Kuroda et al. 2016), so in this case, one would focus on star-forming galaxies for the follow-up. de Mink & Belczynski (2015) argue that the merger rate of neutron-star binaries correlates with the metal abundance of the galaxy, so the total stellar mass regardless of metallicity would provide a better estimate of this rate than the mass of low- Z stars. We connect these properties to the quantities available

in large galaxy surveys, in particular the broad-band fluxes, through the MUFASA simulations of galaxy formation.

The MUFASA galaxy formation simulations use state of the art hydrodynamics, star formation, and feedback modules that well reproduce the global growth of stellar mass in galaxies (Davé et al. 2016b), as well as their star formation rates (SFRs), gas, and metal properties (Davé et al. 2016a). Of particular relevance here is that MUFASA matches the observed distribution of specific SFRs at low redshifts, which is key since high-sSFR galaxies will be especially good follow-up targets. To obtain galaxy spectra they identify galaxies, assume each member star particle is a single stellar population of a given age and metallicity, and use Flexible Stellar Population Synthesis (Conroy et al. 2009; Conroy & Gunn 2010). to compute its spectrum assuming a Chabrier (2003) initial-mass function. They dust attenuate each stellar spectrum based on the extinction computed from the metal column density along the line of sight to that star, assuming a Calzetti et al. (2000) extinction law. MUFASA thus also predicts the distribution of galaxies as a function of absolute magnitude in the 2MASS bands, star-formation rate, stellar mass and mass of low-metallicity stars, which we take as the total mass of star particles in each galaxy with $Z < 0.01Z_{\odot}$, and also the correlations among these quantities because MUFASA generates an ensemble of nearly 7,000 galaxies in an co-moving volume of $(50h^{-1}\text{Mpc})^3$. The value of the solar metallicity is $Z_{\odot} = 0.02$. Our choice of the threshold for the definition of a low-metallicity star is somewhat arbitrary. de Mink & Belczynski (2015) study the merger rates from stellar populations with $Z = 0.1Z_{\odot}$ and contrast these with $Z = Z_{\odot}$. We find that the correlations among the galaxies in MUFASA are similar when one uses $Z < 0.001Z_{\odot}$, so the particular choice of the threshold is not important.

Fig. 1 depicts the fraction of galaxies that contain a given fraction of stellar mass, low- Z stellar mass and current star formation as the solid lines. We immediately can see that half of the stellar mass and half of the current star formation within the ensemble reside in just about six percent of the galaxies; therefore, if one can identify which galaxies have the most star formation for example, one could survey only six percent of the galaxies to measure half of the young stars in the local Universe. This is nearly a factor of ten increase in efficiency. The low-metallicity stars in the Universe are spread more fairly among the galaxies, about one-half of the mass of low- Z stars resides in about one-eighth of the galaxies. Here, the increase is just a factor of four.

The question is whether we can use the observable properties of the galaxies, in particular their absolute magnitudes in the 2MASS bands to sort them at least approximately by stellar mass or star formation, so that one can focus the search to survey the bulk of the stellar mass or star formation rapidly. The figure of merit that we will employ is how much more efficiently we can cover half of the total star formation or stellar mass than we could achieve by surveying the galaxies randomly, and how close this efficiency is to the maximum as depicted in Fig. 1. We fit the logarithm of the total stellar masses, total low- Z stellar mass, and total star formation rate of the galaxies within the MUFASA simulations as a linear combination of the 2MASS absolute magnitudes, for example,

$$\log M_* = A_J M_J + A_H M_H + A_K M_K + B. \quad (2)$$

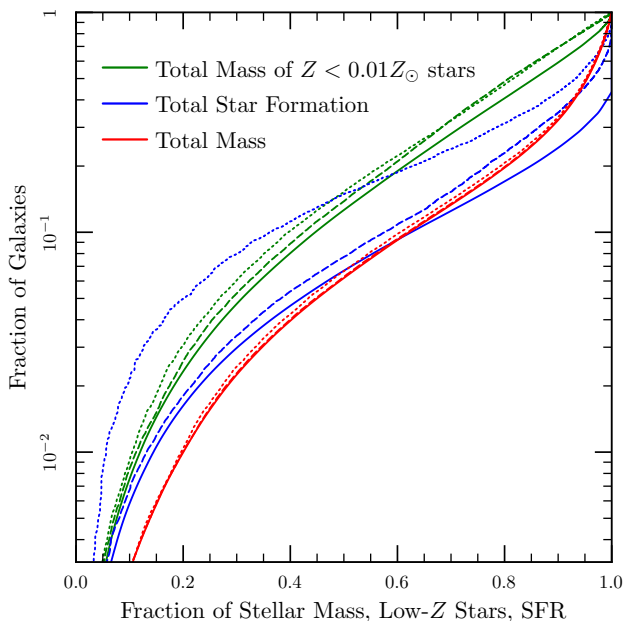


Figure 1. The solid lines traces the minimal fraction of galaxies that contain a given fraction of the total stellar mass, low- Z stellar mass and star formation. The dotted lines show the cumulative fraction if one observes the most luminous galaxies in K_s first. The dashed lines use the values estimated from the 2MASS luminosities to optimize the observing priority.

Table 1. Fitting coefficients for Galaxy Properties

| | A_J | A_H | A_K | B | r |
|-----------------------|-------|-------|-------|-------|------|
| Stellar Mass | 1.87 | -4.07 | 1.79 | 0.75 | 0.98 |
| Low- Z Stellar Mass | -1.81 | 0.05 | 1.53 | 3.43 | 0.97 |
| Star Formation | -3.88 | 6.87 | -3.19 | -2.66 | 0.78 |

The coefficients for the various fits are given in Tab. 1 along with the Pearson correlation coefficient r . We have found empirically that the value of r provides a good estimate of effectiveness of the fit to increase the survey efficiency. For the stellar mass, the sum of the coefficients ($A_J + A_H + A_K$) equals -0.41 , so the total stellar mass is essentially proportional to the luminosity of the galaxy in the 2MASS bands, a well-known result and increases most strongly with the increase in the luminosity in the middle H -band. On the other hand, the sum of the coefficients for the other two fits are about -0.2 , indicating that the star formation rate and mass of low- Z stars within a galaxy are slower functions of luminosity, perhaps proportional $L_{2\text{MASS}}^{1/2}$ or equivalently $M_*^{1/2}$. The estimator for low- Z stars favours galaxies that are bluer in the 2MASS bands; among older stellar populations lower metallicities yield bluer stars. Finally, the star formation estimator favours galaxies bright in the J and K bands, tracing the effects of young stars in the first case and dust in the second.

In particular the red curves of Fig. 1 depict the cumulative stellar mass as a function of the fraction of galaxies survey ordered by their fitted mass (dashed curve) as well as their luminosities in the 2MASS bands (dotted curve). By using the fitted mass we can survey half of the stellar mass

by observing only 6.28% of the galaxies; this is only slightly worse than the best possible performance of 6.20%. The fits to the masses using the power-law relations (Eq. 2) from the 2MASS luminosities perform nearly as well as using the masses themselves. The solid line is nearly indistinguishable from the dashed. One can do nearly as well by just using the total K_s luminosity as a proxy for the stellar mass as shown by the dotted lines. The quality of the fit for the low- Z stellar masses is slightly poorer (green curves), but we can still survey half of the low- Z by observing just 14% of the galaxies, nearly a factor of four improvement. In both of these cases, one could achieve nearly as good performance by simply observing the most luminous galaxies first. Although one can increase the efficiency of finding the low- Z stars substantially, the gains are not as large as for the total stellar mass because the low- Z stars are spread more uniformly among the galaxies. If one is undecided whether one wants to survey the entire stellar population or just the low- Z stars, a reasonable strategy would simply to look at the most luminous galaxies first; of course, after observing a given number of galaxies, the completeness of the survey of the low- Z stars would be worse than that of the total stellar mass as shown in Fig. 1.

The situation is somewhat different for the star formation rate which does not correlate as well with the 2MASS luminosities as the other properties do. The blue curves of Fig. 1 show that one can double the efficiency of the search by using the estimated star formation rate instead of simply observing the brightest galaxies first. By using the estimate of the star formation, one could survey half of the recent star formation in the local Universe by just observing 7.7% of the galaxies, a factor of nearly seven improvement relative to an untargeted search. If one simply observed the most luminous galaxies first, one would have to look at 15.8% of the galaxies to survey half of the star formation.

3 RESULTS

To assess the performance of these techniques to create an observing plan, we will focus on two particular redshift ranges. Antolini & Heyl (2016) examine in detail how the results change with the telescope field of view and how they would change with the redshift range. The first redshift range we will consider is $0.03 < z < 0.04$. Fig. 2 presents the density of galaxies, stellar mass, low- Z stellar mass and star-formation in the redshift range using the parameters estimated from the observed 2MASS luminosities in the 2MPZ, and the fits obtained from the MUFASA simulations. The upper panel depicts simply the number density of galaxies on the sky in the 2MPZ (as we examined in Antolini & Heyl 2016). The second panel depicts the stellar mass in the galaxies. It traces the same structures as in the upper panel, but the contrast is higher. Regions of high galaxy density are relatively stronger peaks in the stellar mass distribution. The third panel shows the mass density of low- Z stars. Here the contrast is somewhat in between the galaxy density and the stellar mass density, and furthermore the void regions are less pronounced in the low- Z population. The lowermost panel depicts the star formation rate. This again follows the structure in the uppermost panel. The regions of the highest star formation correspond to regions of

high galaxy density; however, not every high galaxy density region corresponds to a high star formation rate. There is a stochastic element.

Now we will examine how using sky maps weighted by galaxy properties can increase the efficiency of LIGO follow-up. We choose these particular redshift ranges for comparison with the previous results of (Antolini & Heyl 2016). The solid curves in Fig. 3 show the results for a redshift range of $0.03 < z < 0.04$. The constraints from the gravitational-wave detections are likely to be broader. We use the Bayesian probability region calculated by the BAYESTAR algorithm (Singer & Price 2016) from Singer et al. (2014) for a LIGO-only detection, that is, before Virgo is operational. For simplicity, we focus a single field of view that corresponds to $\text{NSIDE} = 64$ for the HEALPIX map (about one degree across). In this redshift range, this corresponds to about 3 Mpc, so even through the gravitational-wave event may be displaced from the galaxy (e.g. Belczynski et al. 2006) by up to 1 Mpc, it is still likely to lie in the same HEALPIX region. This is the same test as in Antolini & Heyl (2016). The improvement by using a galaxy map is substantial. However, the additional gains by using the galaxy properties are modest about 50% except for the star formation rate where using the colours of the galaxies in the 2MPZ one could improve search efficiency by a factor of two.

To understand why the gains are more modest in the 2MPZ survey than in as simulated in § 2, we examine the distribution of galaxies as a function of absolute K_s magnitude in Fig. 4 for the galaxies with $0.03 < z < 0.04$ in the 2PMZ. The luminosities of the galaxies in the catalogue only span a modest range of about two to three magnitudes. The magnitude-limited survey only probes the most luminous galaxies in this redshift range. These galaxies dominate both the total stellar mass and the mass of low- Z stars. On the other hand, the gains for the star formation rate are more substantial because not all luminous galaxies have ongoing star formation, so the 2MASS colours can help select those galaxies where we expect to find star formation and perform a more efficient search. Fig. 4 also depicts the distribution of luminosities in the 2PMZ for a sample of more local galaxies in $0.01 < z < 0.02$. In this sample, the range of luminosities is broader. The cutoff at high luminosity is at approximately the same place, but the sample extends to lower luminosities. In this case we expect the strategies outlined in § 2 to yield stronger gains in efficiency. These observing plans are depicted as dashed lines in Fig. 3. To probe the distribution of low- Z stars, simply following the distribution of the galaxies themselves yields a similar efficiency to using the additional information; however, in this small redshift range, there are only a few nearby galaxies within the LIGO search region and the 2MPZ. On the other hand, if one is interested in the total stellar mass or the star formation rate, the gains are larger as expected from the distribution of galaxy luminosities in the survey. In fact in this local sample, one would have to observe only four fields to probe half of the star formation to compare with ten fields to probe half of the galaxies and eighty fields to probe half of the LIGO integrated probability.

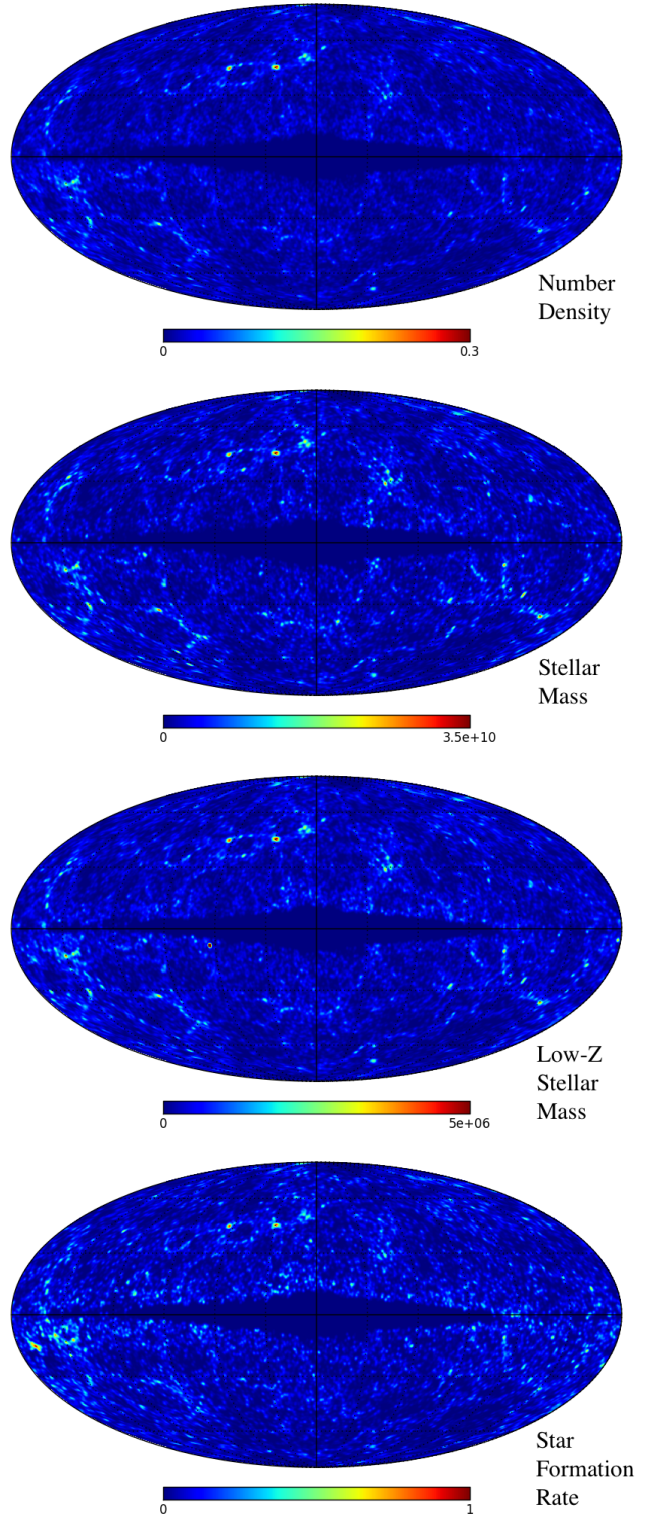


Figure 2. Sky maps of the galaxies with 2MPZ redshifts between 0.03 and 0.04 weighted by from top to bottom number, total stellar mass, total mass of low metallicity stars and current star formation rate, smoothed on a scale of 0.6 degrees. The units are number of galaxies, total stellar mass, total low- Z stellar mass and total mass of stars formed per year within 0.01 square degrees.

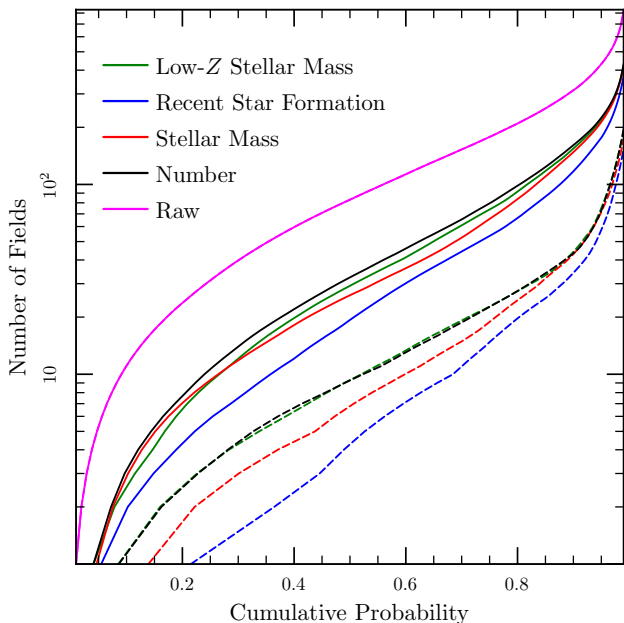


Figure 3. Observing Plans for $0.01 < z < 0.02$ (dashed lines) and $0.03 < z < 0.04$ (solid lines) optimized by low- Z stellar mass, star formation total stellar mass, galaxy density and the raw LIGO probability map.

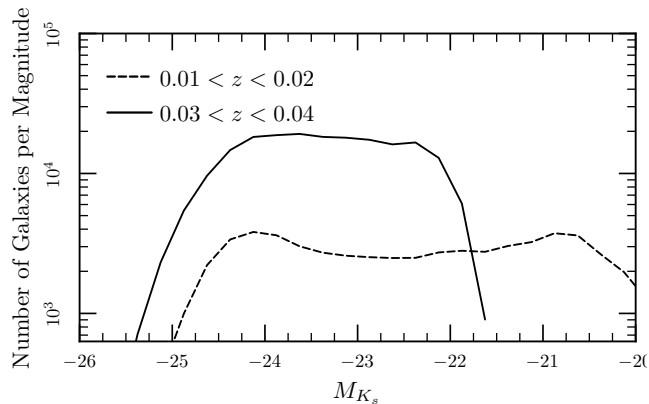


Figure 4. Number of galaxies per unit absolute magnitude for $0.01 < z < 0.02$ (dashed lines) and $0.03 < z < 0.04$ in the 2PMZ.

4 CONCLUSIONS

We have presented a technique to optimize the electromagnetic follow-up observations of gravitational-wave events to focus on the galaxies that are most likely to host the event. In principle this technique can be combined with further optimizations. For example Ghosh et al. (2016) argue that after the highest probability regions are identified, adjusting the positions of the pointings carefully can increase the coverage efficiency by up to 50% over the hundred square-degree search region. Using sky maps weighted by galaxy properties makes the regions of highest probability much more structured, so whether an additional 50% increase in efficiency is possible is not clear. Our strategy can also be complemented by techniques to coordinate multiple telescopes and to ac-

count for the time for the telescope to reach the field or to go from field to field (e.g. Singer et al. 2012).

Rapidly searching for the electromagnetic counterparts to gravitational-wave events is crucial, both because the counterpart may not last long and because the association of a particular electromagnetic transient with the gravitational-wave event becomes less and less significant as time passes. The initial searches for electromagnetic counterparts to the GW150914 event discovered many transients (e.g. Smartt et al. 2016), but it is unlikely that any were associated with the source, both because there were not the expected counterpart and also because the rate of chance associations is so large over the large search in solid angle and time. Strategies as outlined here by reducing the search region increase the chance of finding a counterpart quickly and also reduce the false-coincidence rate.

Acknowledgements

The software and galaxy maps used in this paper are available at <http://ubc-astrophysics.github.io>. We used the VizieR Service, the NASA ADS service, the SuperCOSMOS Science Archive, the NASA/IPAC Infrared Science Archive, the HEALPy libraries and arXiv.org. This work was supported by the Natural Sciences and Engineering Research Council of Canada, the Canadian Foundation for Innovation, the British Columbia Knowledge Development Fund and the Bertha and Louis Weinstein Research Fund at the University of British Columbia.

REFERENCES

- Abbott, B. P. et al. 2016, *Phys. Rev. Lett.*, 116, 061102
 Abbott, B. P. et al. 2016, *Living Reviews in Relativity*, 19
 Antonini, E. & Heyl, J. S. 2016, *Mon. Not. Roy. Ast. Soc.*, 462, 1085
 Bartos, I., Crofts, A. P. S., & Márka, S. 2015, *Astrophys. J. Lett.*, 801, L1
 Belczynski, K., Holz, D. E., Bulik, T., & O’Shaughnessy, R. 2016, *Nature*, 534, 512
 Belczynski, K., Perna, R., Bulik, T., Kalogera, V., Ivanova, N., & Lamb, D. Q. 2006, *Astrophys. J.*, 648, 1110
 Berry, C. P. L. et al. 2015, *Astrophys. J.*, 804, 114
 Bilicki, M., Jarrett, T. H., Peacock, J. A., Cluver, M. E., & Steward, L. 2014, *Astrophys. J. Suppl.*, 210, 9
 Burrows, A. & Hayes, J. 1996, *Physical Review Letters*, 76, 352
 Calzetti, D., Armus, L., Bohlin, R. C., Kinney, A. L., Koornneef, J., & Storchi-Bergmann, T. 2000, *Astrophys. J.*, 533, 682
 Cerioli, A., Lodato, G., & Price, D. J. 2016, *Mon. Not. Roy. Ast. Soc.*, 457, 939
 Chabrier, G. 2003, *Publ. Ast. Soc. Pac.*, 115, 763
 Conroy, C. & Gunn, J. E. 2010, *Astrophys. J.*, 712, 833
 Conroy, C., Gunn, J. E., & White, M. 2009, *Astrophys. J.*, 699, 486
 Davé, R., Rafieferantsoa, M. H., Thompson, R. J., & Hopkins, P. F. 2016a, *Mon. Not. Roy. Ast. Soc.*, submitted (arXiv:1610.01626)
 Davé, R., Thompson, R., & Hopkins, P. F. 2016b, *Mon. Not. Roy. Ast. Soc.*, 462, 3265
 de Mink, S. E. & Belczynski, K. 2015, *Astrophys. J.*, 814, 58

- Dominik, M. et al. 2015, *Astrophys. J.*, 806, 263
- D’Orazio, D. J., Levin, J., Murray, N. W., & Price, L. 2016, *Phys. Rev. D*, 94, 023001
- East, W. E., Paschalidis, V., Pretorius, F., & Shapiro, S. L. 2016, *Phys. Rev. D*, 93, 024011
- Fernández, R. & Metzger, B. D. 2016, *Annual Review of Nuclear and Particle Science*, 66, 23
- Gerosa, D., Kesden, M., O’Shaughnessy, R., Klein, A., Berti, E., Sperhake, U., & Trifirò, D. 2015, *Physical Review Letters*, 115, 141102
- Ghosh, S., Bloemen, S., Nelemans, G., Groot, P. J., & Price, L. R. 2016, *Astron. Astrophys.*, 592, A82
- Hanna, C., Mandel, I., & Vousden, W. 2014, *Astrophys. J.*, 784, 8
- Jarrett, T. H., Chester, T., Cutri, R., Schneider, S., Skrutskie, M., & Huchra, J. P. 2000, *Astron. J.*, 119, 2498
- Kasliwal, M. M. & Nissanke, S. 2014, *Astrophys. J. Lett.*, 789, L5
- Kawaguchi, K., Kyutoku, K., Shibata, M., & Tanaka, M. 2016, *Astrophys. J.*, 825, 52
- Kuroda, T., Kotake, K., & Takiwaki, T. 2016, *Astrophys. J. Lett.*, 829, L14
- Kyutoku, K., Ioka, K., Okawa, H., Shibata, M., & Taniguchi, K. 2015, *Phys. Rev. D*, 92, 044028
- Margalit, B. & Piran, T. 2015, *Mon. Not. Roy. Ast. Soc.*, 452, 3419
- Mingarelli, C. M. F., Levin, J., & Lazio, T. J. W. 2015, *Astrophys. J. Lett.*, 814, L20
- O’Shaughnessy, R., Bellovary, J. M., Brooks, A., Shen, S., Governato, F., & Christensen, C. R. 2017, *Mon. Not. Roy. Ast. Soc.*, 464, 2831
- Ott, C. D. 2009, *Classical and Quantum Gravity*, 26, 063001
- Sasaki, M., Suyama, T., Tanaka, T., & Yokoyama, S. 2016, *Phys. Rev. Lett.*, 117, 061101
- Siegel, D. M. & Ciolfi, R. 2016a, *Astrophys. J.*, 819, 14
- . 2016b, *Astrophys. J.*, 819, 15
- Singer, L., Price, L., & Speranza, A. 2012, *ArXiv e-prints*, 1204.4510
- Singer, L. P. & Price, L. R. 2016, *Phys. Rev. D*, 93, 024013
- Singer, L. P. et al. 2014, *Astrophys. J. Suppl.*, 211, 7
- . 2016, *Astrophys. J. Lett.*, 829, L15
- Skrutskie, M. F. et al. 2006, *Astron. J.*, 131, 1163
- Smartt, S. J. et al. 2016, *Mon. Not. Roy. Ast. Soc.*, 462, 4094
- Yang, H. & Zhang, F. 2016, *Astrophys. J.*, 817, 183